ELSEVIER

Contents lists available at ScienceDirect

Journal of Hazardous Materials

journal homepage: www.elsevier.com/locate/jhazmat



Magnetic surfactant-modified clay for enhanced adsorption of mixtures of per- and polyfluoroalkyl substances (PFAS) in snowmelt: Improving practical applicability and efficiency

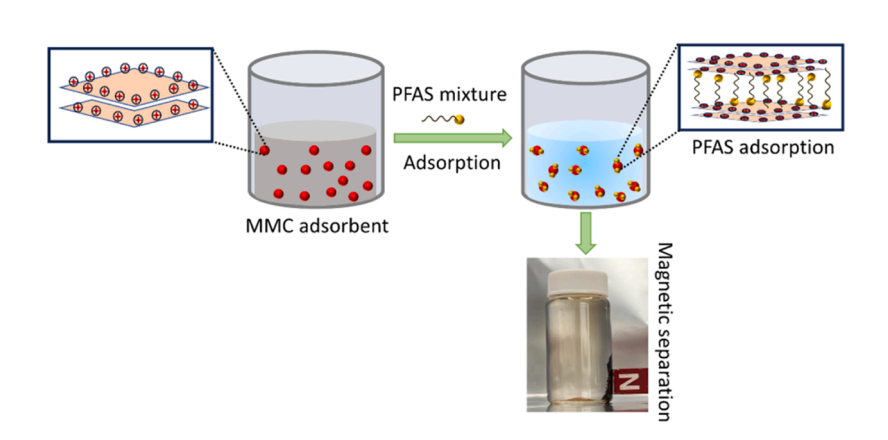
Tao Jiang ^a, Md. Nahid Pervez ^{a,*}, Aswin Kumar Ilango ^a, Yukesh Kannah Ravi ^b, Weilan Zhang ^a, Jeremy I. Feldblyum ^c, Mehmet V. Yigit ^c, Haralabos Efstathiadis ^d, Yanna Liang ^a

- a Department of Environmental and Sustainable Engineering, University at Albany, State University of New York, Albany, New York 12222, United States
- b Centre for Organic and Nanohybrid Electronics, Silesian University of Technology, Konarskiego 22B, 44–100 Gliwice, Poland
- ^c Department of Chemistry, University at Albany, State University of New York, Albany, New York 12222, United States
- d Department of Nanoscale Science and Engineering, University at Albany, State University of New York, Albany, New York 12222, United States

HIGHLIGHTS

- Magnetic modified clay (MMC) exhibits excellent PFAS adsorption performance.
- MMC has good magnetic separation properties to avoid secondary pollution.
- PFAS removal efficiency of MMC is better than that of PAC in the snowmelt metrics.
- MC' regenerability and reusability ensure practical applicability.

G R A P H I C A L A B S T R A C T



ARTICLE INFO

Keywords:

Per- and polyfluoroalkyl substances (PFAS) Adsorption Magnetic modified clay Regeneration and reuse Snowmelt

$A\ B\ S\ T\ R\ A\ C\ T$

The extensive use of per- and polyfluoroalkyl substances (PFAS) in many industrial and consumer contexts, along with their persistent nature and possible health hazards, has led to their recognition as a prevalent environmental issue. While various PFAS removal methods exist, adsorption remains a promising, cost-effective approach. This study evaluated the PFAS adsorption performance of a surfactant-modified clay by comparing it with commercial clay-based adsorbents. Furthermore, the impact of environmental factors, including pH, ionic strength, and natural organic matter, on PFAS adsorption by the modified clay (MC) was evaluated. After proving that the MC was regenerable and reusable, magnetic modified clay (MMC) was synthesized, characterized, and tested for removing a wide range of PFAS in pure water and snowmelt. The MMC was found to have similar adsorption performance as the MC and was able to remove > 90% of the PFAS spiked to the snowmelt. The superior and

^{*} Correspondence to: 1400 Washington Avenue, Albany, NY 12222, USA. E-mail address: mpervez@albany.edu (Md.N. Pervez).

1. Introduction

Per- and polyfluoroalkyl substances (PFAS) encompass a vast array of synthetic organic compounds where the carbon backbones are either fully or partially fluorinated [1,2]. The distinctive characteristics of PFAS have facilitated their extensive utilization in various industrial operations and consumer goods, such as surfactants for mining and oil wells [3,4], coatings for textiles and food packaging [5,6], foams for aqueous film formation [7,8], cosmetics and personal care items [9], cleaning agents [10], and numerous other applications [11]. PFAS, which have been in production for more than six decades and are now widely detected, are recognized as posing high risks to human health and the environment [12–14]. Hence, innovative solutions for eliminating PFAS from the environment are of utmost importance.

Several approaches have been examined for treating PFAS, encompassing physical adsorption/filtration, chemical/electrochemical destruction, and biological degradation [15]. Adsorption is a cost-effective and efficient method for rapidly removing PFAS from polluted water sources. Adsorbents used for PFAS removal primarily consist of carbon-based materials [16,17], ion exchange resins [18,19], biosorbents [20-22], and clay-based materials [23,24]. Activated carbons (ACs), such as granular and powdered AC (GAC and PAC), carbon nanotubes (CNTs), and biochar, are widely recognized as the primary carbon-based materials utilized for the adsorption of PFAS [20,25-27]. Among these materials, PAC and CNTs have demonstrated notable efficacy in adsorption capacity [28,29]. The hydrophobic adsorption of PFAS is facilitated by the presence of non-polar functional groups in carbon-based adsorbents [30]. In contrast to long-chain PFAS, the adsorption of short-chain PFAS presents a distinct challenge due to their increased hydrophilicity and reduced affinity with adsorbents.

Clay-based materials represent an additional classification of adsorbents for PFAS. Numerous investigations have been conducted on the adsorption of PFAS using a diverse range of naturally occurring clays, including montmorillonite (Mt) [24,31], kaolinite [24,31], alumina [32], boehmite [33], and hematite [24]. Nevertheless, the surfaces of natural clays exhibit hydrophilic properties due to the hydration of inorganic cations at the exchange sites. This hydration process leads to a negative charge on the clay surfaces, reducing their efficiency in adsorbing hydrophobic and anionic PFAS [30]. As a result, the adsorption of PFAS is enhanced by modifying natural clays with surfactants, thereby converting the hydrophilic surface to a lipophilic one [34]. Generally, after modification by cationic surfactants, the positively charged surfaces tend to capture anionic PFAS due to electrostatic interactions [35,36]. Mt, belonging to the smectite group, exhibits a structural arrangement consisting of two tetrahedral silicate layers enclosing an aluminum oxide/hydroxide layer (referred to as a 2:1 layered structure) [37]. This configuration facilitates a significant cation exchange capacity (CEC) and specific surface area [38,39]. Previous research has utilized quaternary ammonium compounds to modify the surface of Mt to enhance its ability to adsorb PFAS. In a study conducted by Zhou et al. [23], modifications to Mt using the cationic surfactant hexadecyltrimethylammonium bromide (HDTMAB) led to adsorption capacities of approximately 62 and 339 mg/g for perfluorooctanoic acid (PFOA) and perfluorooctanesulfonic acid (PFOS), respectively, when the HDTMAB to CEC ratio was 0.5. Wang et al. [40] modified Mt by incorporating quaternary ammonium compounds, specifically L-carnitine and choline, to enhance the adsorption capacity for PFOA, PFOS, undecafluoro-2-methyl-3-oxahexanoic acid (GenX), fluorobutane sulfonate (PFBS). Nevertheless, the complete separation of modified clay particles from an aqueous solution post-adsorption is challenging owing to their limited mechanical stability and pronounced

dispersion.

Magnetic adsorbents derived from clay minerals are of significant scientific interest due to their ability to combine distinctive adsorption properties with the cost-effectiveness of clays. Moreover, these adsorbents offer the advantage of easy and fast separation from an aqueous suspension upon exposure to an external magnetic field. Numerous articles are dedicated to magnetic adsorbents with a matrix composed of bentonite, montmorillonite, kaolin, zeolite, and other clays, which are applied to remove dyes, heavy metals, and pharmaceuticals [41–44]. These adsorbents are generally produced through a coprecipitation technique [45,46]. Magnetite-based clay adsorbents have demonstrated a notable affinity and fast adsorption kinetics in the removal of hazardous metal ions [47]. Furthermore, these adsorbents have shown exceptional performance in engineering research and have been successfully employed in industrial and pilot-scale applications [48–50].

However, there has been a notable absence of research specifically addressing the use of magnetic modified clay (MMC) for the adsorption of PFAS mixtures in real-world environments. Therefore, this study aims to fill this gap by fabricating MMC from the MC we reported already. In our previous publication [34], the MC was shown to have fast removal of all short- and long-chain PFAS, including GenX and precursors, through hydrophobic and electrostatic interactions. Before we started the synthesis of MMC, in order to gain more confidence in the MC's adsorption performance and capacity, the MC was tested against a few commercially available clay-based adsorbents. In addition, the effect of environmental parameters, such as pH, ionic strength, and natural organic matter, on MC's adsorption behavior was evaluated as well. This is followed by assessing its regenerability and reusability. Only after we were fully convinced that the MC was a superior and robust adsorbent for PFAS did we embark on the synthesis of MMC, which is followed by structural characterization, understanding its adsorption performance in pure water, snowmelt, and against PAC. Results from this study indicate that the MMC is a much better adsorbent than PAC with regard to removing a range of PFAS in real water samples.

2. Materials and methods

2.1. Chemical reagents and snow samples

The details about the chemical reagents used in this work are shown in Table S1. The physicochemical features of PFAS examined in this research are displayed in Table S2. The snow was collected from the University at Albany, State University of New York grounds in March 2023 and stored at 4 $^{\circ}$ C. The composition of the snowmelt is listed in Table S3.

2.2. Synthesis of modified clay and magnetic modified clay

2.2.1. Synthesis of modified clay

The detailed procedure for synthesizing the modified clay (MC) used in this study has been described in a previous publication [34]. Briefly, a two-step process was employed, starting with the addition of montmorillonite K10 (Alfa Aesar, Haverhill, MA, USA) to a $\rm Na_2CO_3$ solution and stirring for 3 h. Then, a few drops of concentrated hydrochloric acid were added to the mixture, which was followed by rinsing with deionized (DI) water and drying overnight to generate the unmodified clay. The obtained solids were then mixed with a cetyltrimethylammonium chloride (CTAC) solution at an optimal CTAC/CEC ratio of 0.85 [34] and stirred at 80 $^{\circ}$ C for 2 h. This was followed by rinsing with DI water and drying overnight to produce the MC adsorbent.

2.2.2. Synthesis of magnetic modified clay

The magnetic modified clay (MMC) was prepared in the following way. At first, 4.41 g FeCl $_3$ -6 H $_2$ O was dissolved in 200 mL DI water, to which 4.67 g MC was dispersed. The mixture was ultrasonicated for 10 min. Then, 1.61 g FeCl $_2$ -4 H $_2$ O was dissolved in the obtained dispersion. After heating to 90 °C, the pH was adjusted to $\sim\!10$ with an NH $_4$ OH solution ($\sim\!28\%$) under stirring. The mixture was maintained under the same condition for another 1 h. The solids were then collected and rinsed carefully using DI water until the pH reached neutrality. The solids were dried at 90 °C overnight and stored for further use. The magnetic property of MMC can be seen in Videos S1 and S2.

2.3. Adsorption experiments

The adsorption studies were conducted in a batch manner and were replicated three times using 50-mL polypropylene centrifuge tubes (Corning Inc., Corning, NY, USA). To each tube, a PFAS mixture consisting of nine short- and long-chain perfluoroalkyl acids (PFAAs) (C6-C11 perfluorocarboxylic acids (PFCAs) and C4, C6, C8 perfluorosulfonic acids (PFSAs)), GenX, 6:2 fluorotelomer sulfonic acid (6:2 FTSA), and 2-N-ethyl perfluorooctane sulfonamido acetic acid (N-EtFOSAA) was added. The starting concentration for each PFAS was 10 µg/L, and the dose of each adsorbent was 100 mg/L. All tubes with or without an adsorbent were agitated at 150 rpm at room temperature. Subsamples were collected at seven time points: 0, 1, 2, 4, 8, 24, and 48 h. After centrifugation, the supernatant was filtered through 0.2 µm nylon syringe filters, and PFAS were analyzed using an Agilent Technologies 1290 Infinity II LC system paired with a 6470 Triple Quad Mass Spectrometer (LC-MS/MS, Santa Clara, CA, USA). Additionally, the adsorption of PFAS in snowmelt was investigated using a similar methodology, except that each PFAS was spiked at 1, 5, or 10 µg/L. Furthermore, a comparison of adsorption performance was conducted between the MC, MMC, and five commercially available adsorbents (Figure S1), namely FS, FS-F, MAT, MAT-P, and REMPAC (Calgon Carbon, Pittsburgh, PA, USA). The FS, FS-F, MAT, and MAT-P are clay-based adsorbents and REMPAC is powdered activated carbon. FS, FS-F, MAT, and MAT-P have wide particle size ranges, which were determined by the sieving method. The size distribution of these four adsorbents was provided in Table S4. REMPAC has a particle size of 10.21 \pm 2.56 μm and an estimated surface area ranging from 600 to 800 m²/g based on the manufacturer's information. The specific surface areas of MC, MMC, FS, FS-F, MAT, and MAT-P were determined as 13 [34], 48, 1, 4, 40, and 833 m^2/g , respectively, by the Brunauer-Emmett-Teller (BET) method at an activation temperatures of 100 °C.

Moreover, the impacts of three environmental factors, including pH (2, 5, 7, 9, and 12), natural organic matter (NOM) (0, 2, 5, 10, 20, 50, and 100.mg/L humic acid), and ionic strength (0, 5, 10, 50, 100, and 200.mM NaCl) were evaluated on the adsorption of PFAS by both unmodified and modified clays with an initial concentration of $100.\mu\text{g/L}$ for each PFAS mentioned above. The adsorption duration was 4.h.

2.4. Isotherm modeling

The adsorption isotherms of the magnetic modified clay were evaluated using the PFAS mixture consisting of the nine PFAAs, GenX, 6:2 FTSA, and N-EtFOSAA. PFAS solutions were prepared at five concentrations, i.e., 10, 20, 50, 200, and $600.\mu g/L$ for each PFAS, in snowmelt without pH adjustment to simulate the natural environment of stormwater, in which the adsorption process of PFAS by MMC in stormwater was expected to be predicted by the obtained isotherm models. The dose of MMC was 100.mg/L. Samples were collected for PFAS analysis initially and at 48.h when the adsorption process reached equilibrium. Three commonly used isotherm models, i.e., Langmuir, Freundlich, and Sips, were applied to fit the adsorption data, as shown in Eqs. (1) - (3), respectively:

Langmuir:
$$q_e = q_m K_L C_e / (1 + K_L C_e)$$
 (1)

Freundlich:
$$q_e = K_F C_e^{1/m}$$
 (2)

Sips:
$$q_e = q_m (K_S C_e)^{1/n} / (1 + (K_S C_e)^{1/n})$$
 (3)

where q_e and q_m (mg/g) represent the equilibrated adsorbate amount and the theoretical adsorption capacity, respectively; C_e (µg/L) denotes the equilibrated adsorbate concentration in the aqueous phase; K_L (L/µg), K_F (mg·L^{1/m}/(g·µg^{1/m})), and K_S (L/µg) are Langmuir, Freundlich, and Sips isotherm constants, respectively; m is a dimensionless coefficient characterizing the favorability of the adsorption process; and n is a dimensionless parameter qualitatively accounting for the heterogeneity of the adsorbate-sorbent system.

2.5. Regeneration and reuse

In the regeneration step, 5 mL of methanol with 0.1 M NH₄OH was added to the spent MC. The mixture was vortexed for 30 s, sonicated at 35 °C for 30 min, and centrifuged at 4500 rpm for 10 min. The supernatant was then collected. The above extraction steps were repeated twice, and the extract for each round was 5 mL. The residual solids were rinsed using DI water thrice and dried at 90 °C overnight. The solids generated from the recovery step were mixed and reacted with a CTAC solution because of the loss of CTAC in the extraction steps, rinsed with DI water, and dried in an oven, as detailed above. The regenerated adsorbent was then used to remove a PFAS mixture according to the aforementioned steps to investigate its reusability performance.

2.6. Characterization of adsorbents

The Fourier transform infrared spectroscopy (FTIR; PerkinElmer Spectrum 100, Waltham, MA, USA) was used to analyze the functional groups in the adsorbent samples both before and after PFAS adsorption. The spectral data were collected within the 4000-650 cm⁻¹ spectral region, with a resolution of 1 cm⁻¹. To understand adsorbents' surface morphology and elemental composition, a scanning electron microscope (SEM; Zeiss LEO 1550, Oberkochen, Germany) equipped with energy dispersive X-ray spectroscopy (EDS; Bruker Quantax XFlash 6, Billerica, MA, USA) was used. The spent MMC samples for FTIR and SEM-EDS analyses were generated following the adsorption of the 12 aforementioned PFAS at a concentration of 2 mg/L, each with an adsorbent dose of 500 mg/L for 48 h. The crystal structure of the samples was examined using a powder X-ray diffractometer (XRD; Rigaku MiniFlex 6 G, Rigaku Corporation, Tokyo, Japan). The particle size distribution and zeta potential were quantified using a Malvern Zetasizer Nano-ZS analyzer (Malvern Panalytical Ltd, Malvern, UK) at a neutral pH and room temperature.

2.7. Chemical analysis

PFAS in the melted snow were quantified following EPA Method 537.1. Briefly, a surrogate of 30 μL (30 ng, 1 mg/L) $^{13}\text{C-per-fluorohexanoic}$ acid (PFHxA) was spiked to each sample of 400 mL. The spiked sample was then loaded into a Hypersep C_{18} cartridge conditioned by methanol and DI water. Following elution of the PFAS retained on the C_{18} cartridges and before measurement, the samples were supplemented with $^{13}\text{C-PFOS}$ and $^{13}\text{C-PFOA}$ as internal standards. Quantification of the target PFAS in the prepared samples was performed using the Agilent LC-MS/MS. Supernatant samples derived from the adsorption tests were subject to a similar analysis, except that the solid phase extraction (SPE) step was eliminated. Details on PFAS measurements using the LC-MS/MS were reported in the prior reports [13,16,51–53] and presented in Text S1 and Tables S5 and S6.

The anions in the snowmelt were analyzed using a 930 Compact IC Flex instrument (Metrohm, Herisau, Switzerland) equipped with a conductivity detector. Anions were separated using a Metrosep SUPP 5 column (Metrohm). The elution process included the use of a 1:1 combination of 1.8 mM Na $_2$ CO $_3$ and 1.7 mM NaHCO $_3$ as the eluent, with a flow rate of 0.7 mL/min. Subsequently, a solution of H $_2$ SO $_4$ with a concentration of 0.05 M was used as a regenerating agent to mitigate the conductivity. A standard mixture (Thermo Fisher Scientific Inc., USA) consisting of six anions, including Cl $_5$, F $_7$, Br $_7$, SO $_4$, NO $_3$, and PO $_4$ was employed to build calibration curves in the range of 1–500 µg/L. Total nitrogen (TN) was analyzed using a TNT 828 kit on a Hach spectrophotometer (DR 3900, Loveland, CO, USA). Total organic carbon (TOC) was determined by a Shimadzu TOC-L analyzer (Columbia, MD, USA).

3. Results and discussion

3.1. Comparison of PFAS adsorption performance in pure water between modified clay and commercial clay-based adsorbents

To compare the adsorption performance of MC with those of commercially available clay-based adsorbents, namely FS, FS-F, MAT, and MAT-P, PFAS concentrations in the subsamples collected at 1, 4, 8, and 48 h were measured, and PFAS' removal efficiencies were calculated as shown in Fig. 1. The main observation is that MC had excellent adsorption performance in terms of adsorption rate, i.e., almost 100% removal within 1 h for all 12 PFAS. No desorption occurred for MC, at

least in the studied time interval of 1-48 h, confirming the strong binding of MC with all target PFAS compounds. In contrast, in addition to the low adsorption rate of the commercial clay adsorbents, desorption of some PFAS from all four commercial adsorbents occurred as time increased (Fig. 1). For instance, FS showed desorption for PFDA, perfluoroundecanoic acid (PFUnA), PFOS, 6:2 FTSA, and N-EtFOSAA. The enhanced adsorption performance of MC compared to commercial adsorbents may be attributed to a combination of factors, including the unique two-step process with pretreatment of Mt and the specific use of CTAC at an optimal CTAC/CEC ratio of 0.85 for modification. The primary objective of the pretreatment process of Mt with a Na₂CO₃ solution was to remove impurities and replace the dominant exchangeable metal ions, such as Al³⁺, Fe³⁺, and Ca²⁺ [54], with Na⁺. The Na-Mt was produced in this process with predominant exchangeable metal ions in the form of Na⁺. The rationale behind this process lies in the ease with which Na⁺ ions on the Na-Mt can be exchanged with the target intercalatant, i.e., CTA⁺. The pretreatment served as a purification step, minimizing the interference of unwanted metal ions and enhancing the selectivity of the clay for CTA⁺.

3.2. Impacts of environmental factors on adsorption of PFAS by modified clay

For this purpose, PFAS each at $100~\mu g/L$ was tested given the consideration that no impact by different environmental factors may be captured if the concentration of each PFAS was $10~\mu g/L$ as shown in Fig. 1.

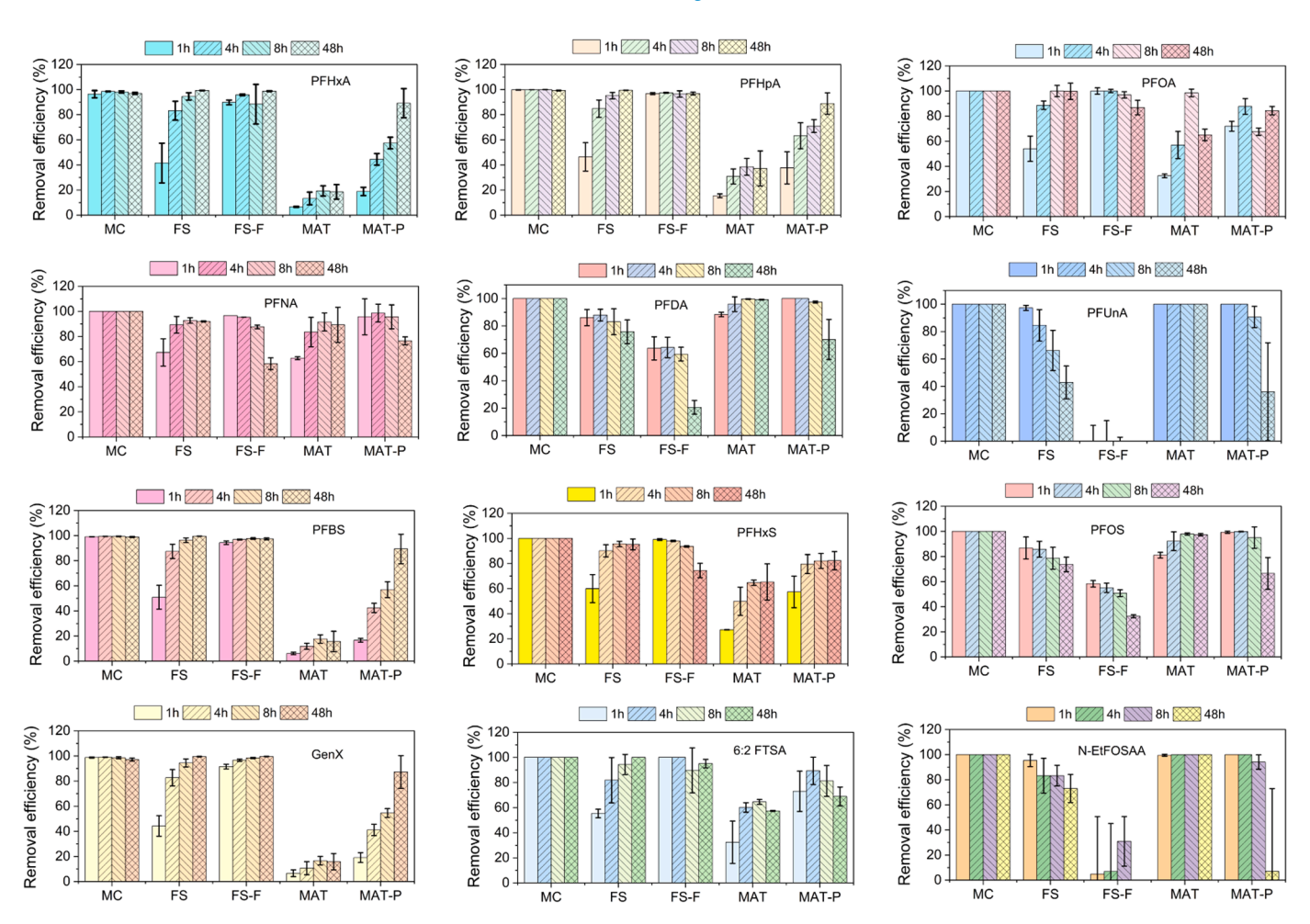


Fig. 1. . Adsorption performance comparison among modified clay and commercially available clay-based adsorbents for PFAS at different contact times (1, 4, 8, and 48 h). The initial concentration of each tested PFAS was 10 μ g/L, and the dose of each adsorbent was 100 mg/L. The solution pH was unadjusted (~5.5). Error bars represent the standard deviations of triplicate measurements.

3.2.1. pH effect

The impact of varying pH levels (2, 5, 7, 9, and 12) on the adsorption of PFAS by both unmodified clay and MC was explored. As shown in Fig. 2a and b, both clays displayed pH sensitivity in their adsorption behavior. The unmodified clay exhibited limited adsorption capabilities for all examined PFAS, suggesting that the clay's intrinsic properties alone were not sufficient to effectively remove PFAS from aqueous solutions [34]. As pH changed, removal efficiencies remained low for most PFAS. In contrast, the modification of clay significantly enhanced its adsorption capacity for PFAS across all pH levels. Notably, at pH of 2 and 5, MC achieved nearly complete removal for most PFAS. As pH increased, the removal efficiency showed a decreasing trend in general. This can be attributed to: 1) competition from anions. At pH of 9, the concentration of OH was 0.01 mM. The molar concentration of PFAS at 100 µg/L was much lower. In the case of PFOS, it was 0.0002 mM, 50 times lower than that of OH⁻; and 2) the reduced surface charges of MC as pH increased [34]. In particular, the surface of MC became negatively charged as the pH rose to 10. The less positive and even negative surface charges of MC at high pH levels could significantly reduce the adsorption of tested PFAS due to their negative charges. Previous studies have also shown that more positive surface charges of adsorbents were beneficial for PFAS adsorption [34,55,56]. The results also showed that the impacts of pH on PFAS adsorption were dependent on the chain

length of PFAS, exhibiting a more significant impact on short-chain PFAS. Especially, as pH increased, removal efficiencies for short-chain PFAS, including PFHxA, perfluoroheptanoic acid (PFHpA), PFBS, and GenX, were dramatically reduced, while the impacts were slight for the adsorption of long-chain PFAS, such as perfluorononanoic acid (PFNA), perfluorodecanoic acid (PFDA), PFOS, and N-EtFOSAA.

3.2.2. Ionic strength effect

The influence of ionic strength on PFAS adsorption by both unmodified clay and MC was also investigated at varying NaCl levels (Fig. 2c and d). The ionic strength exhibited a generally negative effect on the adsorption of PFAS by both clays. For the unmodified clay, as the ionic strength increased, removal efficiencies of all PFAS decreased, even resulting in nearly no removal for some PFAS, such as PFOS and PFDA. This indicated the highly negative impact of ionic strength on the adsorption performance of unmodified clay for all PFAS, regardless of their chain lengths and functional groups. Conversely, the increasing ionic strength only affected the adsorption of short-chain PFAS, i.e., PFHXA, PFHPA, PFBS, and GenX for the modified clay. For the long-chain PFAS, no obvious impacts were observed. This resilience to ionic strength fluctuations underscored the potential of MC as a robust solution for efficient PFAS removal under diverse environmental conditions, with implications for practical remediation strategies.

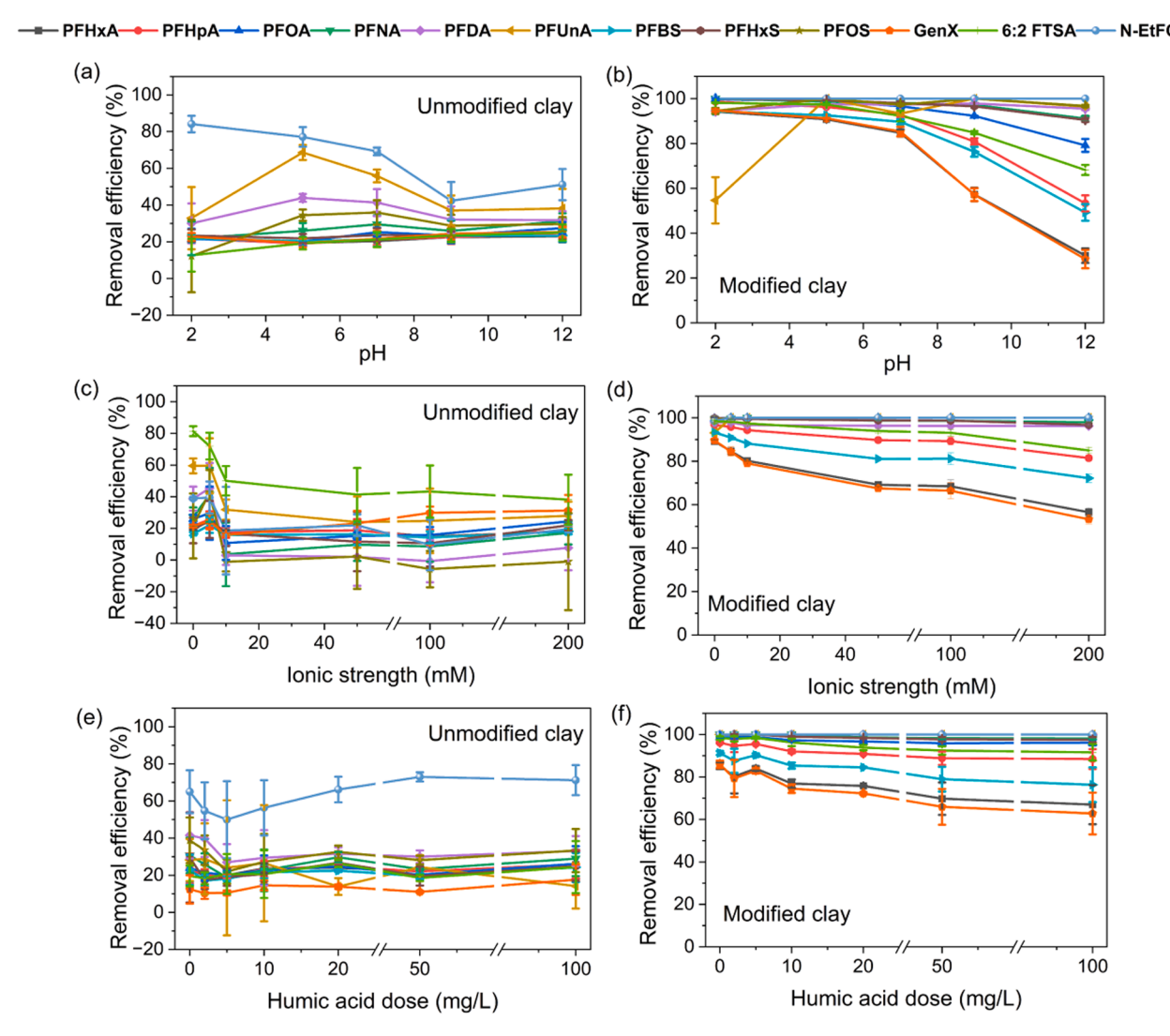


Fig. 2. Effects of environmental factors on adsorption of PFAS by unmodified and modified clays. The initial concentration of each tested PFAS was 100 μ g/L, and the dose of each adsorbent was 100 μ g/L. The solution pH was unadjusted (\sim 5) in c-f. The adsorption duration was 4 h. Error bars represent the standard deviations of triplicate measurements.

3.2.3. Natural organic matter effect

NOM, represented by humic acid, showed an evident impact on the PFAS adsorption performance of both unmodified clay and MC (Fig. 2e and f). This phenomenon was more pronounced for the unmodified clay, where increasing humic acid generally led to reduced removal efficiencies for all PFAS, except N-EtFOSAA, suggesting competition between humic acid and PFAS for adsorption sites on the unmodified clay surface. MC consistently demonstrated good adsorption performance across all tested humic acid doses. Even in the presence of high NOM levels, the MC maintained nearly complete removal of all long-chain PFAS. This suggested that the clay modification process enhanced its affinity for PFAS, allowing it to effectively compete with humic acid for adsorption sites. This finding suggested that the MC held promise for effective PFAS remediation in natural waters where NOM is commonly present.

3.3. Regeneration and reuse of modified clay

Despite the widespread use of adsorption processes for PFAS removal, one of their full-scale application's main drawbacks is the difficulty of regenerating the spent materials when their adsorption capacity has been exhausted. Regeneration must allow the nearly

complete removal of adsorbed PFAS to restore the adsorption capacity of the spent materials through technologies that have economic viability and environmental security [57]. For this purpose, this study conducted three rounds of extraction by basic methanol (0.1 M NH₄OH) at room temperature. As shown in Fig. 3a, all adsorbed PFAS were recovered after three rounds of extraction with the first round recovering the majority. The regenerated MC was found to have similar adsorption performance as the original MC (Fig. 3b). Thus, the MC can be regenerated and reused repeatedly.

3.4. Adsorption of PFAS by magnetic modified clay in pure water

Although MC has excellent and super-fast adsorption performance for all target PFAS, its powder form brings an issue of separation when it is used in suspension. To facilitate the separation of MC from water, MMC was synthesized by adding the magnetic property. Fig. 4a and Video S2 showed that MMC can be separated fast and easily in water by a magnetic bar. The adsorption of a mixture of 12 PFAS by MMC was tested in pure water. As shown in Fig. 4b, at an initial individual concentration of $10~\mu g/L$, the adsorption of all PFAS reached a high removal efficiency (> 89%) within 1 h. Specifically, for the four short-chain PFAS, i.e., PFHxA, PFHpA, PFBS, and GenX, removal efficiencies

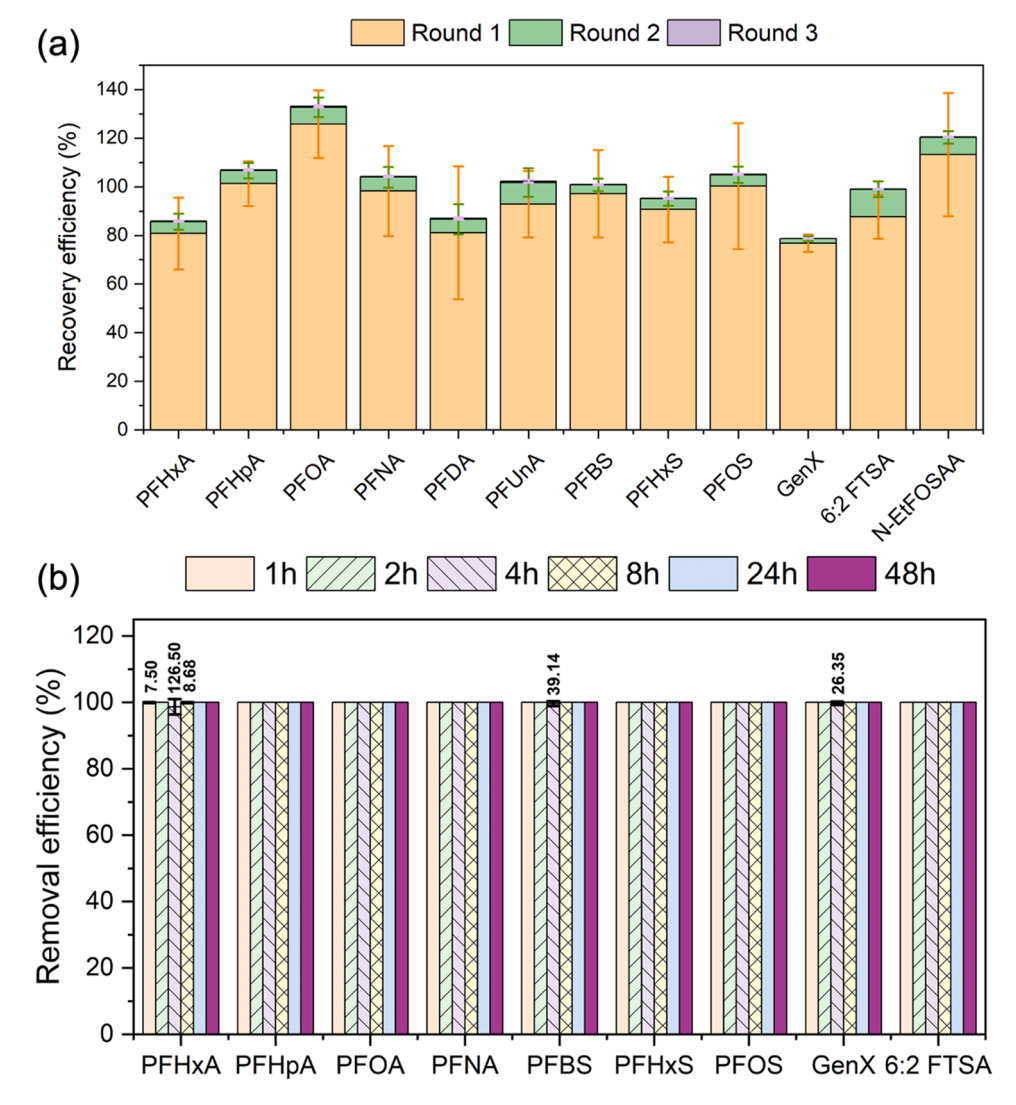


Fig. 3. (a) Recovery of MC and (b) Reuse MC for PFAS adsorption. The initial concentration of each tested PFAS was 10 μg/L, and the dose of adsorbent was 100 mg/L. The solution pH was unadjusted (~5.5). Error bars represent the standard deviations of triplicate measurements. The numbers above the error bars are the residual concentrations in ng/L. The absence of a number indicates a residual concentration lower than the limit of detection for each PFAS shown in Tables S5 and S6.

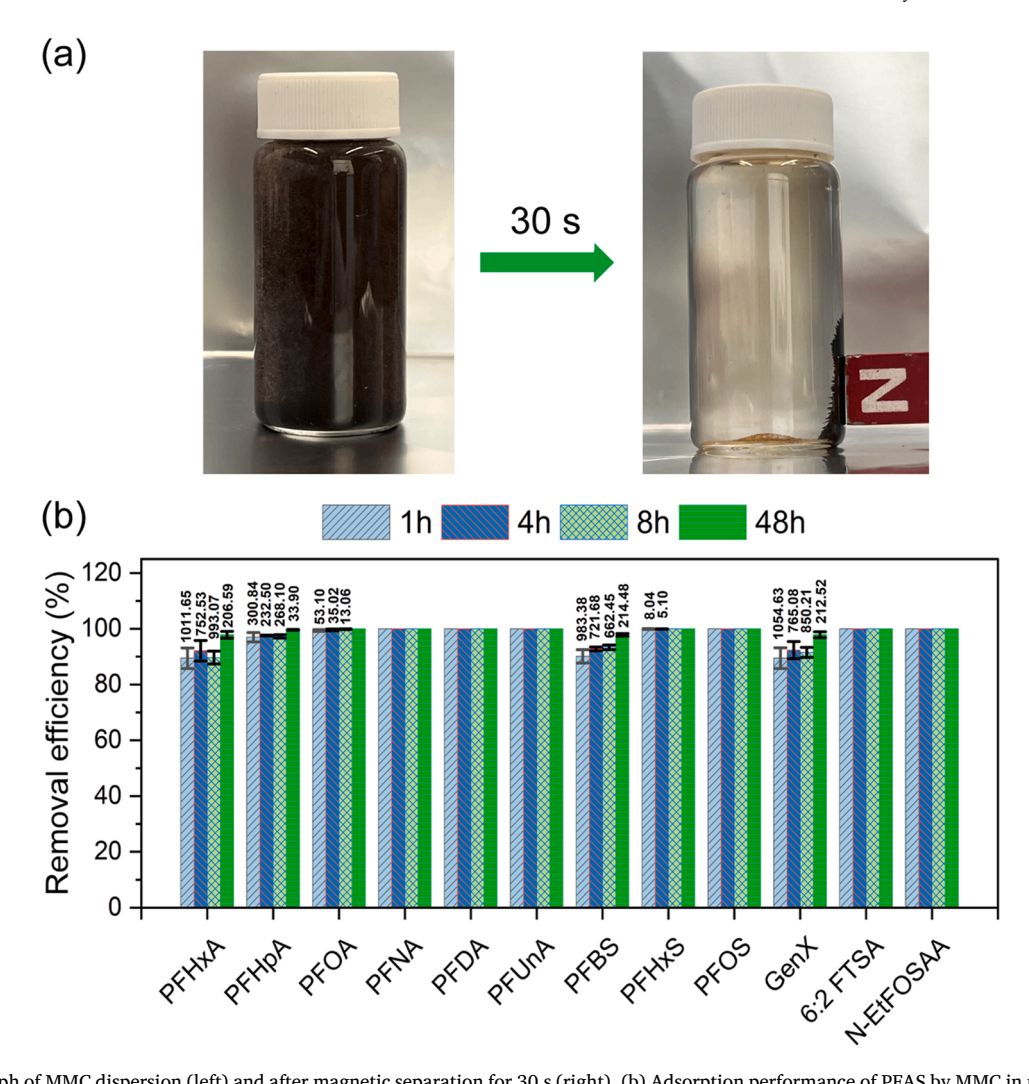


Fig. 4. (a) Photograph of MMC dispersion (left) and after magnetic separation for 30 s (right). (b) Adsorption performance of PFAS by MMC in pure water. The initial concentration of each tested PFAS was $10 \mu g/L$, and the dose of adsorbent was 100 mg/L. The solution pH was unadjusted (\sim 5.5). Error bars represent the standard deviations of triplicate measurements. The numbers above the error bars are the residual concentrations in ng/L. The absence of a number indicates a residual concentration lower than the limit of detection for each PFAS shown in Tables S5 and S6.

ranged from 89.4% to 97.0% within 1 h and kept rising to nearly 100% as the contact time increased to 48 h. In comparison, for the six long-chain PFCAs (C8-C11) and PFSAs (C7-C8), as well as 6:2 FTSA and N-EtFOSAA, saturated adsorption was attained with almost 100% removal efficiency within the initial hour and no desorption was observed during the exposure duration of 48 h. These findings underscored the excellent adsorption performance of MMC for both short- and long-chain PFAS. Additionally, in comparison with previously documented magnetic

PFAS adsorbents, the MMC exhibited comparable or better performance for PFAS adsorption, as shown in Table 1. This suggested that MMC could serve as a highly effective adsorbent for PFAS in water.

3.5. Characterization of magnetic modified clay

3.5.1. Morphological and physicochemical properties SEM-EDS was utilized to examine the morphology and elemental

 Table 1

 Adsorption performance of the synthesized MmC in the present study with the magnetic PFAS adsorbents reported in the literature.

Adsorbent	Adsorbent dose	Contact time (h)	Initial concentration of each PFAS	Tested PFAS and removal (%)	Reference
Magnetic ion-exchange resin ^a	4 mL/L	2	300 ng/L	PFBA: ~20, PFPeA: ~25, PFHxA: ~44, PFHpA: ~62, PFOA: ~67, PFDA: ~90, PFBS: ~78, PFOS: ~90, PFOS branched: ~91	Park et al.,[58]
Magnetic fluorinated polymer ^a	500 mg/L	24	100 μg/L	PFBA: ~82, PFPeA: ~97, PFHxA: ~99, PFHpA: ~100, PFOA: ~100, PFNA: ~99, PFDA: ~99, PFBS: ~100, PFHxS: ~99, PFOS: ~99, GenX: ~99	Tan et al.,[59]
Fe ₃ O ₄ -cyclodextrin-ionic liquid magnetic nanoparticles	50 mg/L	24	50 μg/L	PFOA: 93, PFOS: 99	Badruddoza et al.,[60]
MMC ^b	100 mg/L	48	10 μg/L	PFHxA: 97.84 \pm 1.21, PFHpA: 99.66 \pm 0.11, PFOA: ~100, PFNA: ~100, PFDA: ~100, PFUnA: ~100, PFBS: 97.84 \pm 0.51, PFHxS: ~100, PFOS: ~100, GenX: 97.87 \pm 1.11, 6:2 FTSA: ~100, N-EtFOSAA: ~100	This study

Note: a: the PFAS removal (%) values were estimated from the figures in the references. b: the PFAS removal (%) values are average \pm SD (standard deviation).

composition of the MMC before and after PFAS adsorption. The adsorption was performed for 12 PFAS each at 2 mg/L with an MMC dose of 500 mg/L for 48 h. As shown in Fig. 5a and b, before adsorption, sizable particles were agglomerated and possessed irregular shapes. The EDS analysis indicated that oxygen (O), iron (Fe), silicon (Si), and aluminum (Al) were the predominant elements, constituting more than 90% of the overall elemental compositions. These findings aligned with previous research [61,62] regarding the structural formula of Mt.

Following the adsorption process, the adsorbent surface became heterogeneous because of the hydraulic forces during the agitation and showed the presence of mineral and crystalline phases. The metallic elements Fe, Al, and Ti were present on the surface of the MMC, as seen in Fig. 5c and d. The presence of empty spaces inside the interparticle cavities among the smaller particles resulted in the formation of macroporous structures in the larger aggregated clay particles. These structures are believed to have a notable impact on the adsorption of PFAS by promoting the movement of the adsorbate through the cavities. Besides, the principal elements exhibited minor fluctuations due to the exchange of ions between PFAS compounds and water molecules coordinated with Fe [63]. Moreover, the existence of PFAS on the MMC can be seen based on the EDS spectrum, which identified the presence of fluorine (F) (3.99%) originating from the adsorbed PFAS, as shown in Fig. 5c and d.

The surface of MC was positively charged [34], and the zeta potential of MMC was determined to be 11.13 mV. This observation suggested that the process of magnetic modification did not compromise the positively charged property of the adsorbent surface, which was

beneficial for PFAS adsorption. Furthermore, it was observed that the particle size underwent a reduction after the magnetic modification process, with values of $5.40\pm0.83~\mu m$ for MC and $3.59\pm0.21~\mu m$ for MMC. In general, the physicochemical features of MMC indicated its suitability for use in environmental matrices where PFAS are often found to possess a negative charge. Previous research has also shown that adsorbents with a greater positive charge and smaller particle size have a greater affinity for adsorbing PFAS [55,56].

3.5.2. FTIR

The functional groups of the pristine and spent MMC were investigated using FTIR. As shown in Fig. 6a, the FTIR spectra of MMC showed a minute band at 3391 cm⁻¹ associated with the stretching vibration of the O-H (adsorbed water) in the CTAC and clay layer, while the bending vibrations of O-H were observed at 1644 cm⁻¹ [64]. The strong stretching vibrations of Si-O functional groups of the MC in MMC appeared at 1019 cm⁻¹ [65]. Next, the minute FTIR bands at 580-560 cm⁻¹ were attributed mainly to the stretching vibrations of Fe-O and are typical of magnetite [66,67]. The main observations in the FTIR spectra of PFAS-laden MMC were: 1) FTIR bands of MMC reappeared with altered signals, and a few new bands appeared due to PFAS adsorption; 2) The stretching vibration of Fe-O almost disappeared after PFAS adsorption due to the interactions between Fe³⁺ and anionic head groups such as COO and SO3 of PFAS; 3) The FTIR band intensity in the stretching vibration of C-H hydrophobic segment of MMC at 2925 cm⁻¹ was affected slightly suggesting the minor hydrophobic interactions between MMC and PFAS molecules; 4) The new FTIR bands at 1365 and

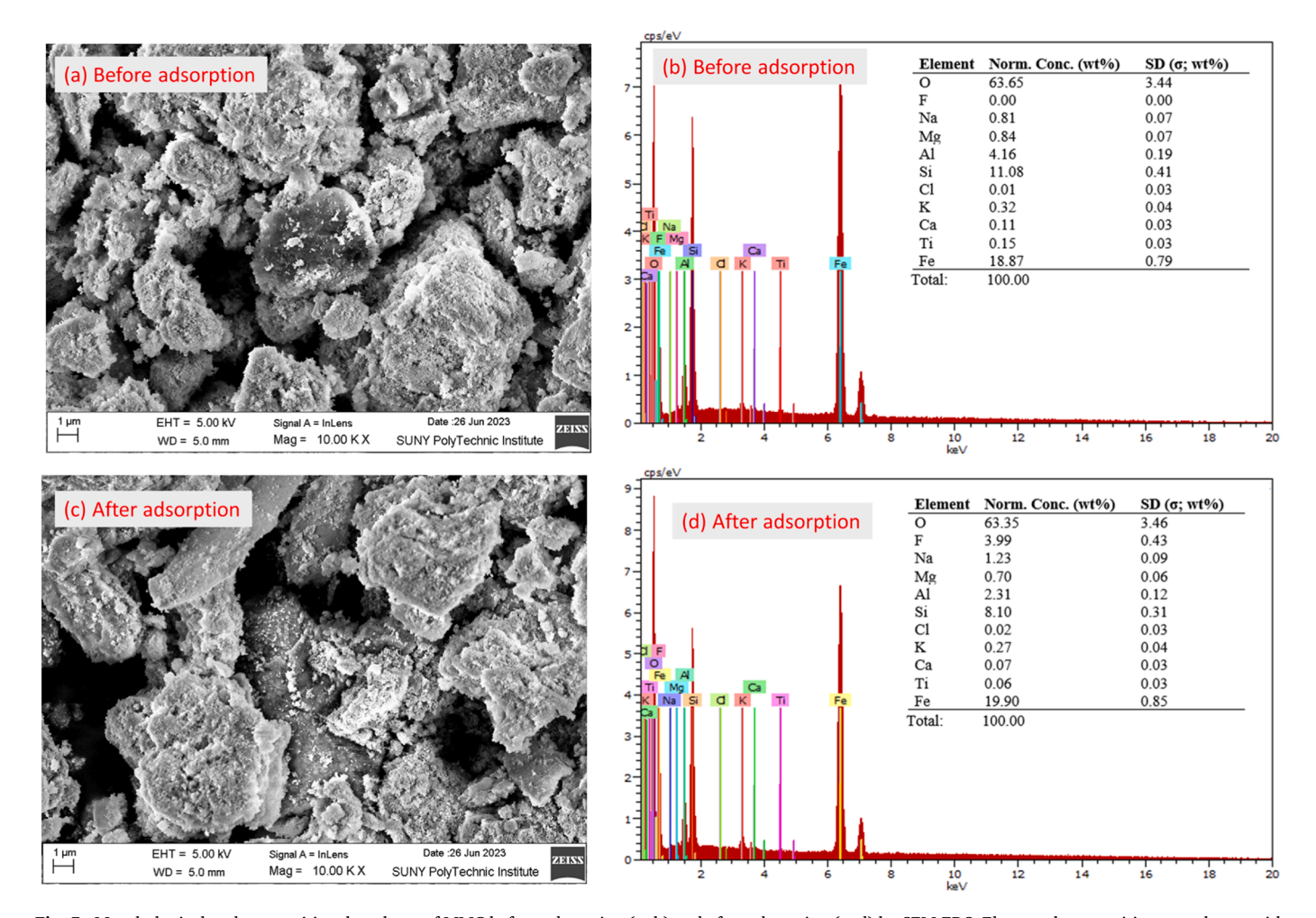


Fig. 5. Morphological and compositional analyses of MMC before adsorption (a, b) and after adsorption (c, d) by SEM-EDS. Elemental compositions are shown with normalized concentrations (wt%) and standard deviations (SD).

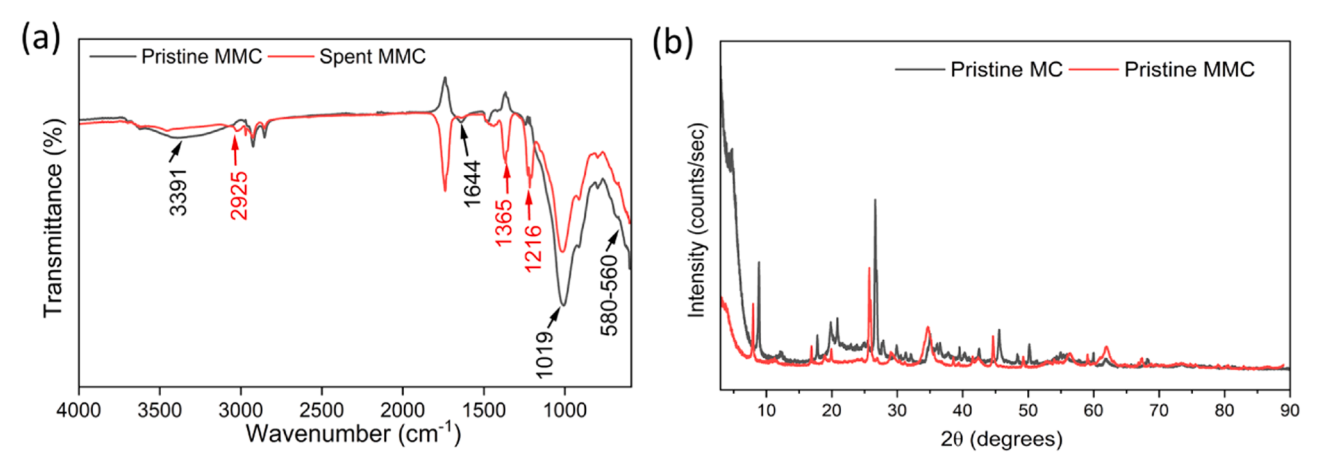


Fig. 6. (a) FTIR spectra of pristine and spent MMC; (b) XRD pattern of pristine MC and pristine MMC.

 $1216~\rm cm^{-1}$ corresponded to the stretching vibrations of -CF $_2$ - and -CF $_3$ groups from organic fluorine [22,68], indicating the strong interactions of the PFAS compounds with MMC.

3.5.3. XRD

XRD analysis of the MC and MMC is illustrated in Fig. 6b. In the XRD pattern of MC, the main characteristic reflection peak of the montmorillonite crystalline structure was observed at $2\theta=8.87^\circ$, corresponding to the inter-layer spacing (d) of 0.99 nm [69]. The same characteristic peak also appeared in the magnetite loaded MC (MMC) at $2\theta=8.95^\circ$ (d =0.98 nm). The interlayer space at $2\theta=9^\circ$ was not affected by the magnetic particles. Several other XRD peaks attributed to different impurities were detected in the MC and MMC diffractogram, which can be omitted.

3.6. Adsorption of PFAS by magnetic modified clay in snowmelt

To assess the efficacy of MMC more precisely in practical scenarios, experiments were conducted to evaluate its adsorption of PFAS in snowmelt. The findings indicated that a rapid adsorption process occurred during the first hour of contact time, as seen in Fig. 7. At the starting concentrations of 1 and 5 μ g/L, the adsorption process reached its maximum within 1 h with removal efficiencies for all PFAS between 90% and 100% (Fig. 7). With an initial concentration of 10 μ g/L for each PFAS, the effect of carbon chain length on adsorption was observed. Notably, PFAS with longer carbon chains exhibited higher removal than their short-chain counterparts, which aligned with the results reported previously [70].

In snowmelt, the short-chain PFAS, including PFHxA, PFBS, and GenX, exhibited incomplete adsorption in 8 h and had removal efficiencies varying between 84% and 96%. The adsorption performance of the material was slightly lower than that in pure water, as seen in Fig. 4, with a range of 89.4% to 97%. This observation implied that the presence of chemicals in snowmelt has a negative effect on the performance of the adsorbents. The chemical analysis of snowmelt indicated the presence of two types of anions, namely bromide at $64.43 \pm 0.72 \, \mu g/L$ and phosphate at 17.72 \pm 1.28 $\mu g/L$ (Table S3). Besides, the studied snowmelt contained a higher content of TN (0.10 \pm 0.10 mg/L) and TOC (31.34 \pm 2.28 mg/L) compared to other types of precipitation, such as rainwater and stormwater [71,72]. The TOC, in particular, is much higher than the global mean content of TOC in lake water at 5.578 mg/L [73]. Anions and TOC are known to compete for the adsorption sites with PFAS and negatively impact the effectiveness of adsorption [56,57]. Our findings, thus, exhibited a significant correlation with prior studies that have shown a reduced efficacy in the removal of PFAS in natural water [74,75]. Given the small decrease in removal efficiency of MMC for PFAS in snowmelt, the MMC reported in this study

has great potential in capturing PFAS in aquatic environments.

A comparative analysis was conducted to assess the adsorption efficiency of MMC in snowmelt, in parallel with PAC (REMPAC from Calgon Carbon), which is a commonly used commercial adsorbent in practical applications. According to Fig. 7, PAC exhibited lower adsorption performance than MMC for all PFAS at the lower concentration level (1 ppb) in terms of both adsorption rate and efficiency during the 8-h contact period, while their performance was comparable at the higher concentration levels (5 and 10 ppb). Therefore, MMC would be a better option compared to PAC for removing PFAS in snowmelt, at least in suspension systems. Compared to other adsorbents, MMC was also proven superior in terms of PFAS removal from natural precipitation medium (Table 2).

3.7. Isotherms of PFAS adsorption by magnetic modified clay

To establish isotherm models of Langmuir, Freundlich, and Sips, the total q_e and C_e values for all PFAS were calculated and applied, due to the low individual PFAS C_e values that were near or below the detection limit for lower concentration levels and long-chain PFAS, as well as the similar adsorption mechanism probably shared among all tested PFAS [34]. The Langmuir model accounts for dynamic adsorption-desorption equilibrium, the Freundlich model describes adsorption processes on heterogeneous surfaces, and the Sips model integrates both isotherms to predict adsorption in heterogeneous systems [61]. As depicted in Fig. 8, the Langmuir model demonstrated a good fit to the experimental adsorption data in the high concentration range and the Sips isotherm exhibited strong fits in the low range, while the Freundlich model accurately captured the entire range of data with the highest coefficient of determination (R^2) (Table 3). The best fitting of the adsorption data to Freundlich isotherm suggested that hydrophobic interactions might be the dominant adsorption mechanism at both low and high concentrations, due to the strong association of Freundlich isotherm with hydrophobic interactions [78]. This adsorption mechanism was different from that of MC, for which hydrophobic interactions and electrostatic interactions were probably governing mechanisms at low and high concentrations, respectively [34]. This discrepancy was supported by the relatively lower positive surface charge of MMC than MC.

4. Conclusions

This study systematically examined the adsorption performance of MC for a diverse mixture of PFAS, demonstrating that MC exhibited exceptional adsorption capabilities, achieving nearly complete removal of PFAS within one hour. Importantly, MC maintained a relatively high adsorption performance, especially for long-chain PFAS, under various environmental conditions, including changes in pH, ionic strength, and

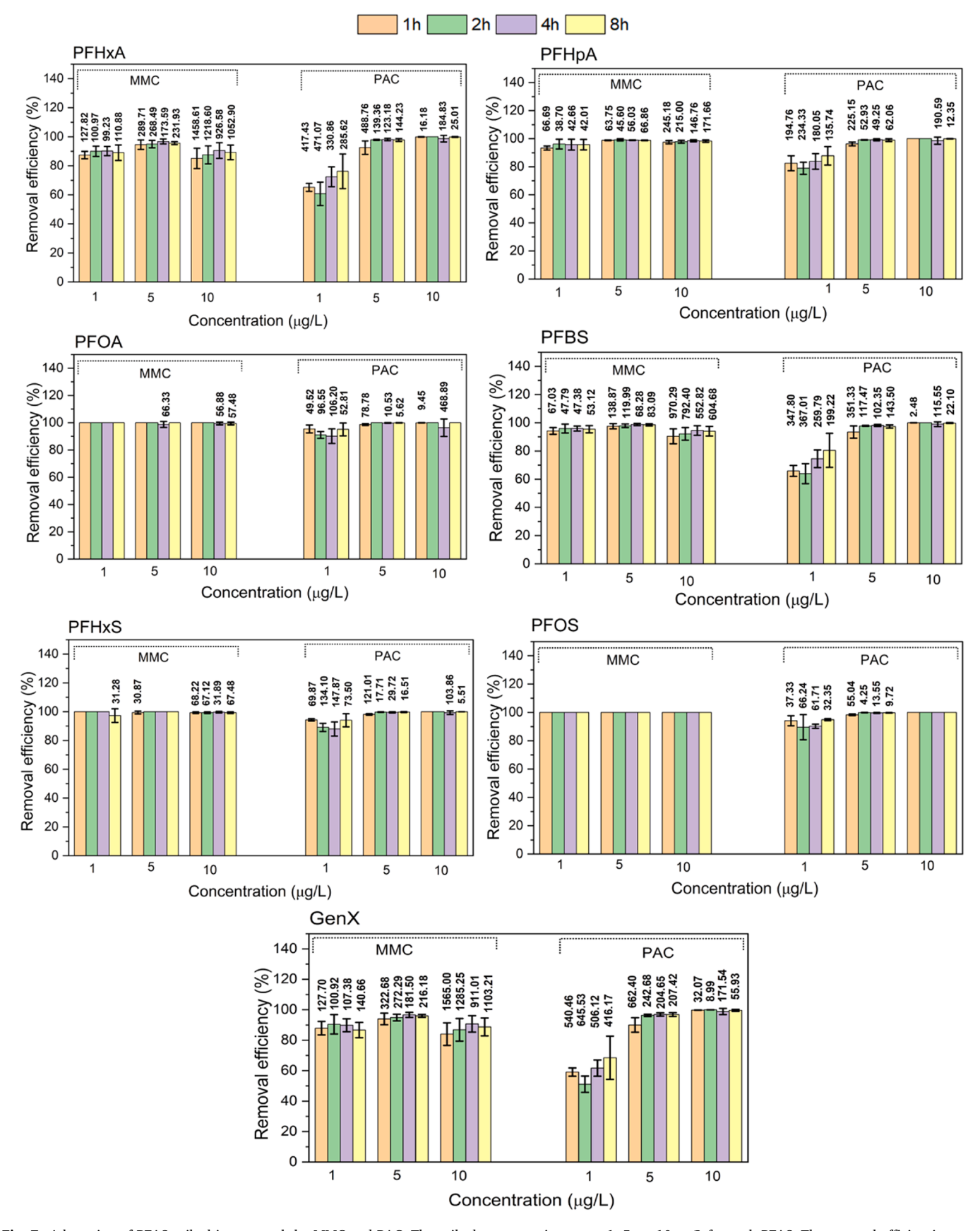


Fig. 7. Adsorption of PFAS spiked in snowmelt by MMC and PAC. The spiked concentrations were 1, 5, or $10 \,\mu\text{g/L}$ for each PFAS. The removal efficiencies were calculated based on the measured concentrations which might be slightly different from the spiked ones. The dose of each adsorbent was $100 \, \text{mg/L}$. The solution pH was unadjusted. Error bars represent the standard deviations of triplicate measurements. The numbers above the error bars are the residual concentrations in ng/L. The absence of a number indicates a residual concentration lower than the limit of detection for each PFAS shown in Tables S5 and S6.

Table 2Comparison of adsorption performance of MMC in the removal of PFAS in precipitation with reported data.

Adsorbent/Filter	Medium	Adsorbent dose (mg/L)	Contact time (h)	Initial concentration of each PFAS (µg/L)	Tested PFAS and removal (%)	Reference
Biochar Basic ^a EarthLite ^a	Stormwater	40	24	1	PFOA: 6.5 ± 14.7 , PFHxS: 4.8 ± 14 , PFOS: 1.8 ± 19.2 PFOA: 28 ± 17 , PFHxS: 27 ± 4.4 , PFOS:	Parker et al., [74]
Calgon F400 ^a					55 ± 20 PFOA: 28 \pm 5, PFHxS: 81 \pm 17, PFOS: 64	
RemBind ^a					\pm 3 PFOA: 95 \pm 3, PFHxS: 84 \pm 7, PFOS: 91 \pm 4	
Poly(diallyldimethylammonium) chloride (PDADMAC)-clay ^b	Stormwater	500	24	5 50 500	PFOA: ~99, PFOS: ~90 PFOA: ~97, PFOS: ~99 PFOA: ~95, PFOS: ~99	Ray et al., [76]
$\begin{array}{c} Poly(\text{4-vinylpyridine-co-styrene)-} \\ clay^b \end{array}$				5 5 50 500	PFOA: ~99, PFOS: ~96 PFOA: ~97, PFOS: ~99 PFOA: ~90, PFOS: ~99	
Biochar ^b				5 5 50 500	PFOA: ~99, PFOS: ~99 PFOA: ~99, PFOS: ~99 PFOA: ~99, PFOS: ~99	
Biofilter with PDADMAC ^b	Stormwater	10,000 mg/L PDADMAC was injected to biofilter at 2 mL/min	-	500	PFBA: ~90, PFHxA: ~90, PFOA: ~100, PFDA: ~98	Borthakur et al.,[77]
PAC ^c	Snowmelt	100	8	1	PFHxA: 76.19 ± 11.95 , PFHpA: 87.79 ± 6.52 , PFOA: 95.09 ± 4.73 , PFBS: 80.43 ± 12.09 , PFHxS: 94.03 ± 4.55 , PFOS: 94.88 ± 0.71 , GenX: 68.48 ± 14.19	This study
				5	PFHxA: 97.78 ± 1.01 , PFHpA: 98.97 ± 0.93 , PFOA: 99.90 ± 0.17 , PFBS: 97.31 ± 1.20 , PFHxS: 99.74 ± 0.38 , PFOS: 99.70 ± 0.20 , GenX: 96.86 ± 1.26	
				10	PFHxA: 99.82 ± 0.31 , PFHpA: 99.90 ± 0.16 , PFOA: ~ 100 , PFBS: 99.81 ± 0.33 , PFHxS: 99.96 ± 0.07 , PFOS: ~ 100 , GenX: 99.61 ± 0.66	
MMC ^c				1	PFHxA: 89.02 ± 5.35, PFHpA: 95.73 ± 3.73, PFOA: ~100, PFBS: 95.43 ± 2.53, PFHxS: 97.26 ± 4.73, PFOS: ~100, GenX: 86.67 ± 5.01	
				5	PFHxA: 95.63 ± 1.01, PFHpA: 98.74 ± 0.25, PFOA: ~100, PFBS: 98.52 ± 0.75, PFHxS: ~100, PFOS: ~100, GenX: 95.95 ± 0.95	
				10	FFHxA: 89.20 ± 5.03, PFHpA: 98.25 ± 0.86, PFOA: 99.40 ± 1.02, PFBS: 94.01 ± 3.42, PFHxS: 99.30 ± 0.60, PFOS: ~100, GenX: 88.72 ± 5.87	

Note: a: the PFAS removal (%) values are average \pm 95 CI (confidence interval). b: the PFAS removal (%) values were estimated from the figures in the references. c: the PFAS removal (%) values are average \pm SD.

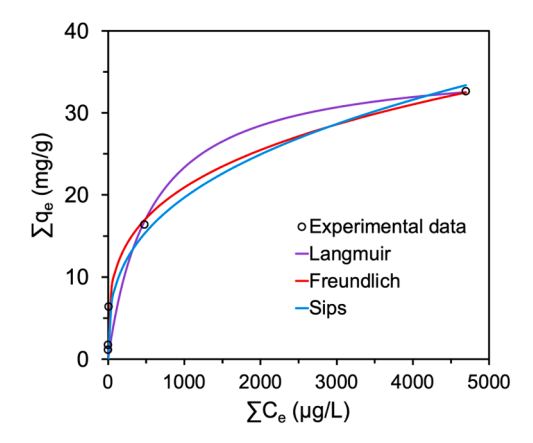


Fig. 8. Isotherms of Langmuir, Freundlich, and Sips models for the adsorption of total PFAS by the magnetic modified clay. Experimental data represent the average values obtained from triplicate measurements.

Table 3Parameters and values obtained from adsorption isotherm models of Langmuir, Freundlich, and Sips for PFAS adsorption by the magnetic modified clay.

Model	Parameter	Value		
Langmuir	R^2	0.9771		
	K_L (L/ μ g)	1.79×10^{-3}		
	$q_m (\text{mg/g})$	36.41		
Freundlich	R^2	0.9965		
	$K_F (\text{mg-L}^{1/m}/(\text{g-}\mu\text{g}^{1/m}))$	2.92		
	m	3.51		
Sips	R^2	0.9953		
	K_S (L/ μ g)	$1.30 imes 10^{-10}$		
	$q_m (\text{mg/g})$	4619.28		
	n	2.91		

the presence of natural organic matter. This robustness positioned MC as a reliable solution for PFAS removal across different water sources and conditions. Furthermore, the regenerability and reusability of MC make it even more attractive as a cost-effective and environmentally friendly PFAS adsorbent.

To enable fast and complete separation of MC from water, magnetic

properties were added to MC, and thus, a new type of adsorbent, MMC, was formed. This study highlighted the potential of MMC in removing PFAS in pure water and snowmelt and demonstrated its superiority to PAC in terms of adsorption efficiency and kinetics. Further research and field testing are warranted to validate the feasibility of using MMC-based systems for removing PFAS in other water matrices at an industrial scale.

Environmental implication

Per- and polyfluoroalkyl substances (PFAS) are a class of pollutants that exhibit persistence, bioaccumulation, and widespread distribution, posing significant risks to human and environmental well-being. This research assessed the efficacy of removing PFAS from aquatic environments. Specifically, the study investigated the adsorption capabilities of a magnetic modified clay material, which has not been previously explored in existing literature. Significantly, it was observed that the prepared adsorbent exhibited superior sorption capabilities for PFAS in snowmelt compared to a commercially available adsorbent, namely powdered activated carbon. This finding eventually presents a promising prospect for environmental sustainability.

CRediT authorship contribution statement

Tao Jiang: Writing – review & editing, Writing – original draft, Visualization, Methodology, Formal analysis, Data curation, Conceptualization. Md. Nahid Pervez: Writing – review & editing, Visualization, Validation, Methodology, Formal analysis, Data curation. Aswin Kumar Ilango: Writing – review & editing, Data curation. Yukesh Kannah Ravi: Writing – review & editing, Data curation. Weilan Zhang: Writing – review & editing, Formal analysis. Jeremy I. Feldblyum: Writing – review & editing, Formal analysis. Mehmet V. Yigit: Writing – review & editing, Formal analysis. Haralabos Efstathiadis: Writing – review & editing, Formal analysis. Yanna Liang: Writing – review & editing, Formal analysis. Yanna Liang: Writing – review & editing, Supervision, Funding acquisition, Conceptualization.

Declaration of Competing Interest

The authors declare that they have no known competing financial interests or personal relationships that could have appeared to influence the work reported in this paper.

Data availability

Data will be made available on request.

Acknowledgments

The authors acknowledge financial support from the U.S. National Science Foundation under award number CBET 2225596 and FuzeHub Jeff Lawrence Innovation Fund (Project number 2022-IC-0000000076) to YL. We appreciate Calgon Carbon for providing REMPAC and anonymous companies for providing the clay-based adsorbents. We are also grateful to Kevin Shah and Yamini Kumaran from UAlbany for their assistance with SEM-EDS measurements, and to Darin Sukalingum from UAlbany for BET analyses.

Appendix A. Supporting information

Supplementary data associated with this article can be found in the online version at doi:10.1016/j.jhazmat.2024.134390.

References

- [1] Evich, M.G., Davis, M.J., McCord, J.P., Acrey, B., Awkerman, J.A., Knappe, D.R., Lindstrom, A.B., Speth, T.F., Tebes-Stevens, C., Strynar, M.J., Wang, Z., 2022. Perand polyfluoroalkyl substances in the environment. Science 375, eabg9065.
- [2] Ehsan, M.N., Riza, M., Pervez, M.N., Khyum, M.M.O., Liang, Y., Naddeo, V., 2023. Environmental and health impacts of PFAS: sources, distribution and sustainable management in North Carolina (USA). Sci Total Environ 878, 163123.
- [3] Murphy, P.M., Hewat, T., 2008. Fluorosurfactants in enhanced oil recovery. Open Pet Eng J 1 (1).
- [4] Meng, Y., Yao, Y., Chen, H., Li, Q., Sun, H., 2021. Legacy and emerging per-and polyfluoroalkyl substances (PFASs) in dagang oilfield: multimedia distribution and contributions of unknown precursors. J Hazard Mater 412, 125177.
- [5] Trier, X., Granby, K., Christensen, J.H., 2011. Polyfluorinated surfactants (PFS) in paper and board coatings for food packaging. Environ Sci Pollut Res 18 (7), 1108–1120.
- [6] Schellenberger, S., Liagkouridis, I., Awad, R., Khan, S., Plassmann, M., Peters, G., Benskin, J.P., Cousins, I.T., 2022. An outdoor aging study to investigate the release of per-and polyfluoroalkyl substances (PFAS) from functional textiles. Environ Sci Technol 56 (6), 3471–3479.
- [7] Dauchy, X., Boiteux, V., Bach, C., Rosin, C., Munoz, J.F., 2017. Per-and polyfluoroalkyl substances in firefighting foam concentrates and water samples collected near sites impacted by the use of these foams. Chemosphere 183, 53–61.
- [8] Leary, D.B., Takazawa, M., Kannan, K., Khalil, N., 2020. Perfluoroalkyl substances and metabolic syndrome in firefighters: a pilot study. J Occup Environ Med 62 (1), 52–57.
- [9] Fujii, Y., Harada, K.H., Koizumi, A., 2013. Occurrence of perfluorinated carboxylic acids (PFCAs) in personal care products and compounding agents. Chemosphere 93 (3), 538–544.
- [10] Kotthoff, M., Müller, J., Jürling, H., Schlummer, M., Fiedler, D., 2015. Perfluoroalkyl and polyfluoroalkyl substances in consumer products. Environ Sci Pollut Res 22 (19), 14546–14559.
- [11] Glüge, J., Scheringer, M., Cousins, I.T., DeWitt, J.C., Goldenman, G., Herzke, D., Lohmann, R., Ng, C.A., Trier, X., Wang, Z., 2020. An overview of the uses of perand polyfluoroalkyl substances (PFAS). Environ Sci: Process Impacts 22 (12), 2345–2373
- [12] Kovarova, J., Svobodova, Z., 2008. Perfluorinated compounds: occurrence and risk profile. Neuroendocrinol Lett 29 (5), 599–608.
- [13] Jiang, T., Zhang, W., Liang, Y., 2022. Uptake of individual and mixed per-and polyfluoroalkyl substances (PFAS) by soybean and their effects on functional genes related to nitrification, denitrification, and nitrogen fixation. Sci Total Environ 838, 156640.
- [14] Jiang, T., Geisler, M., Zhang, W., Liang, Y., 2021. Fluoroalkylether compounds affect microbial community structures and abundance of nitrogen cycle-related genes in soil-microbe-plant systems. Ecotoxicol Environ Saf 228, 113033.
- [15] Leung, S.C.E., Shukla, P., Chen, D., Eftekhari, E., An, H., Zare, F., Ghasemi, N., Zhang, D., Nguyen, N.-T., Li, Q., 2022. Emerging technologies for PFOS/PFOA degradation: a review. Sci Total Environ 827, 153669.
- [16] Zhang, W., Jiang, T., Liang, Y., 2022. Stabilization of per-and polyfluoroalkyl substances (PFAS) in sewage sludge using different sorbents. J Hazard Mater Adv 6, 100000
- [17] Sörengård, M., Östblom, E., Köhler, S., Ahrens, L., 2020. Adsorption behavior of per-and polyfluoralkyl substances (PFASs) to 44 inorganic and organic sorbents and use of dyes as proxies for PFAS sorption. J Environ Chem Eng 8 (3), 103744.
- [18] Boyer, T.H., Fang, Y., Ellis, A., Dietz, R., Choi, Y.J., Schaefer, C.E., Higgins, C.P., Strathmann, T.J., 2021. Anion exchange resin removal of per-and polyfluoroalkyl substances (PFAS) from impacted water: a critical review. Water Res 200, 117244.
- [19] Dixit, F., Dutta, R., Barbeau, B., Berube, P., Mohseni, M., 2021. PFAS removal by ion exchange resins: a review. Chemosphere 272, 129777.
- [20] Chen, X., Xia, X., Wang, X., Qiao, J., Chen, H., 2011. A comparative study on sorption of perfluorooctane sulfonate (PFOS) by chars, ash and carbon nanotubes. Chemosphere 83 (10), 1313–1319.
- [21] Zhang, Q., Deng, S., Yu, G., Huang, J., 2011. Removal of perfluorooctane sulfonate from aqueous solution by crosslinked chitosan beads: sorption kinetics and uptake mechanism. Bioresour Technol 102 (3), 2265–2271.
- [22] Ilango, A.K., Jiang, T., Zhang, W., Feldblyum, J.I., Efstathiadis, H., Liang, Y., 2023. Surface-modified biopolymers for removing mixtures of per-and polyfluoroalkyl substances from water: Screening and removal mechanisms. Environ Pollut 331, 12165.
- [23] Zhou, Q., Deng, S., Yu, Q., Zhang, Q., Yu, G., Huang, J., He, H., 2010. Sorption of perfluorooctane sulfonate on organo-montmorillonites. Chemosphere 78 (6), 698-604
- [24] Zhao, L., Bian, J., Zhang, Y., Zhu, L., Liu, Z., 2014. Comparison of the sorption behaviors and mechanisms of perfluorosulfonates and perfluorocarboxylic acids on three kinds of clay minerals. Chemosphere 114, 51–58.
- [25] Sørmo, E., Silvani, L., Bjerkli, N., Hagemann, N., Zimmerman, A.R., Hale, S.E., Hansen, C.B., Hartnik, T., Cornelissen, G., 2021. Stabilization of PFAScontaminated soil with activated biochar. Sci Total Environ 763, 144034.
- [26] Zhang, D., Zhang, W., Liang, Y., 2019. Adsorption of perfluoroalkyl and polyfluoroalkyl substances (PFASs) from aqueous solution-A review. Sci Total Environ 694, 133606.
- [27] Ilango, A.K., Jiang, T., Zhang, W., Pervez, M.N., Feldblyum, J.I., Efstathiadis, H., Liang, Y., 2023. Enhanced adsorption of mixtures of per- and polyfluoroalkyl substances in water by chemically modified activated carbon. ACS EST Water 3 (11), 3708–3715.

- [28] Sarkar, B., Mandal, S., Tsang, Y.F., Kumar, P., Kim, K.-H., Ok, Y.S., 2018. Designer carbon nanotubes for contaminant removal in water and wastewater: a critical review. Sci Total Environ 612, 561–581.
- [29] Xiao, X., Ulrich, B.A., Chen, B.L., Higgins, C.P., 2017. Sorption of poly- and perfluoroalkyl substances (PFASs) relevant to aqueous film-forming foam (AFFF)impacted groundwater by biochars and activated carbon. Environ Sci Technol 51 (11), 6342–6351.
- [30] Bolan, N., Sarkar, B., Yan, Y., Li, Q., Wijesekara, H., Kannan, K., Tsang, D.C., Schauerte, M., Bosch, J., Noll, H., 2021. Remediation of poly-and perfluoroalkyl substances (PFAS) contaminated soils—To mobilize or to immobilize or to degrade? J Hazard Mater 401, 123892.
- [31] Zhang, R., Yan, W., Jing, C., 2014. Mechanistic study of PFOS adsorption on kaolinite and montmorillonite. Colloids Surf 462, 252–258.
- [32] Wang, F., Shih, K.M., 2011. Adsorption of perfluorooctanesulfonate (PFOS) and perfluorooctanoate (PFOA) on alumina: influence of solution pH and cations. Water Res 45 (9), 2925–2930.
- [33] Wang, F., Liu, C.S., Shih, K.M., 2012. Adsorption behavior of perfluorooctanesulfonate (PFOS) and perfluorooctanoate (PFOA) on boehmite. Chemosphere 89 (8), 1009–1014.
- [34] Jiang, T., Zhang, W., Ilango, A.K., Feldblyum, J.I., Wei, Z., Efstathiadis, H., Yigit, M.V., Liang, Y., 2023. Surfactant-modified clay for adsorption of mixtures of per-and polyfluoroalkyl substances (PFAS) in aqueous solutions. ACS Appl Eng Mater 1 (1), 394–407.
- [35] Sarkar, B., Megharaj, M., Xi, Y.F., Naidu, R., 2011. Structural characterisation of Arquad (R) 2HT-75 organobentonites: surface charge characteristics and environmental application. J Hazard Mater 195, 155–161.
- [36] Sarkar, B., Xi, Y.F., Megharaj, M., Krishnamurti, G.S.R., Bowman, M., Rose, H., Naidu, R., 2012. Bioreactive organoclay: a new technology for environmental remediation. Crit Rev Environ Sci Technol 42 (5), 435–488.
- [37] Uddin, F., 2008. Clays, nanoclays, and montmorillonite minerals. Metall Mater Trans A 39 (12), 2804–2814.
- [38] He, H.P., Guo, J.G., Xie, X.D., Peng, J.L., 2021. Location and migration of cations in Cu2+-adsorbed montmorillonite. Environ Int 26 (5–6), 347–352.
- [39] Zhou, Q., He, H.P., Zhu, J.X., Shen, W., Frost, R.L., Yuan, P., 2008. Mechanism of p-nitrophenol adsorption from aqueous solution by HDTMA(+)-pillared montmorillonite Implications for water purification. J Hazard Mater 154 (1–3), 1025–1032.
- [40] Wang, M.C., Orr, A.A., Jakubowski, J.M., Bird, K.E., Casey, C.M., Hearon, S.E., Tamamis, P., Phillips, T.D., 2021. Enhanced adsorption of per- and polyfluoroalkyl substances (PFAS) by edible, nutrient-amended montmorillonite clays. Water Res 188, 116534.
- [41] Liu, H., Chen, W., Liu, C., Liu, Y., Dong, C., 2014. Magnetic mesoporous clay adsorbent: preparation, characterization and adsorption capacity for atrazine. Microporous Mesoporous Mater 194, 72–78.
- [42] Wang, J., He, D., Chu, L., Zhang, Y., Zhang, W., Zhang, H., 2023. A novel magnetization-modified attapulgite as an excellent adsorbent for tetracycline in water. JOM 75 (12), 5606–5618.
- [43] Shahinpour, A., Tanhaei, B., Ayati, A., Beiki, H., Sillanpää, M., 2022. Binary dyes adsorption onto novel designed magnetic clay-biopolymer hydrogel involves characterization and adsorption performance: kinetic, equilibrium, thermodynamic, and adsorption mechanism. J Mol Liq 366, 120303.
- [44] Zhu, L., Zhu, D., Sheng, Y., Xu, J., Harbottle, D., Zhang, H., 2022. Polydopamine-coated magnetic montmorillonite immobilized with potassium copper hexacyanoferrate for selective removal of Cs+ and its facile recovery. Appl Clay Sci 216. 106367.
- [45] Chang, J., Ma, J., Ma, Q., Zhang, D., Qiao, N., Hu, M., Ma, H., 2016. Adsorption of methylene blue onto Fe3O4/activated montmorillonite nanocomposite. Appl Clay Sci 119, 132–140.
- [46] Magdy, A., Fouad, Y.O., Abdel-Aziz, M.H., Konsowa, A.H., 2017. Synthesis and characterization of Fe3O4/kaolin magnetic nanocomposite and its application in wastewater treatment. J Ind Eng Chem 56, 299–311.
- [47] Shah, K.H., Ali, S., Shah, F., Waseem, M., Ismail, B., Khan, R.A., Khan, A.M., Khan, A.R., 2018. Magnetic oxide nanoparticles (Fe3O4) impregnated bentonite clay as a potential adsorbent for Cr(III) adsorption. Mater Res Express 5 (9), 096102
- [48] Prabhu, S.M., Rane, N.R., Li, X., Otari, S.V., Girawale, S.D., Palake, A.R., Kodam, K. M., Park, Y.K., Ha, Y.H., Kumar Yadav, K., Ali Khan, M., Jeon, B.H., 2023. Magnetic nanostructured adsorbents for water treatment: structure-property relationships, chemistry of interactions, and lab-to-industry integration. Chem Eng J 468, 143474.
- [49] Salinas, T., Durruty, I., Arciniegas, L., Pasquevich, G., Lanfranconi, M., Orsi, I., Alvarez, V., Bonanni, S., 2018. Design and testing of a pilot scale magnetic separator for the treatment of textile dyeing wastewater. J Environ Manag 218, 562-568
- [50] Hassan, M., Naidu, R., Du, J., Liu, Y., Qi, F., 2020. Critical review of magnetic biosorbents: their preparation, application, and regeneration for wastewater treatment. Sci Total Environ 702, 134893.
- [51] Zhang, W., Zhang, Q., Liang, Y., 2022. Ineffectiveness of ultrasound at low frequency for treating per-and polyfluoroalkyl substances in sewage sludge. Chemosphere 286, 131748.
- [52] Zhang, W., Liang, Y., 2022. Performance of different sorbents toward stabilizing per-and polyfluoroalkyl substances (PFAS) in soil. Environ Adv 8, 100217.

- [53] Jiang, T., Pervez, M.N., Quianes, M.M., Zhang, W., Naddeo, V., Liang, Y., 2023. Effective stabilization of per-and polyfluoroalkyl substances (PFAS) precursors in wastewater treatment sludge by surfactant-modified clay. Chemosphere 341, 140081
- [54] Mucha, M., Maršálek, R., Bukáčková, M., Zelenková, G., 2020. Interaction among clays and bovine serum albumin. RSC Adv 10 (72), 43927–43939.
- [55] Pauletto, P.S., Bandosz, T.J., 2022. Activated carbon versus metal-organic frameworks: a review of their PFAS adsorption performance. J Hazard Mater 425, 127810
- [56] Wu, C., Klemes, M.J., Trang, B., Dichtel, W.R., Helbling, D.E., 2020. Exploring the factors that influence the adsorption of anionic PFAS on conventional and emerging adsorbents in aquatic matrices. Water Res 182, 115950.
- [57] Gagliano, E., Sgroi, M., Falciglia, P.P., Vagliasindi, F.G.A., Roccaro, P., 2020. Removal of poly- and perfluoroalkyl substances (PFAS) from water by adsorption: role of PFAS chain length, effect of organic matter and challenges in adsorbent regeneration. Water Res 171, 115381.
- [58] Park, M., Daniels, K.D., Wu, S., Ziska, A.D., Snyder, S.A., 2020. Magnetic ion-exchange (MIEX) resin for perfluorinated alkylsubstance (PFAS) removal in groundwater: roles of atomic charges for adsorption. Water Res 181, 115897.
- [59] Tan, X., Dewapriya, P., Prasad, P., Chang, Y., Huang, X., Wang, Y., Gong, X., Hopkins, T.E., Fu, C., Thomas, K.V., Peng, H., Whittaker, A.K., Zhang, C., 2022. Efficient removal of perfluorinated chemicals from contaminated water sources using magnetic fluorinated polymer sorbents. Angew Chem Int Edition 61 (49), e202213071.
- [60] Badruddoza, A.Z.M., Bhattarai, B., Suri, R.P., 2017. Environmentally friendly β-cyclodextrin-ionic liquid polyurethane-modified magnetic sorbent for the removal of PFOA, PFOS, and Cr (VI) from water. ACS Sustain Chem Eng 5 (10), 9223–9232.
- [61] Yan, B., Munoz, G., Sauvé, S., Liu, J., 2020. Molecular mechanisms of per- and polyfluoroalkyl substances on a modified clay: a combined experimental and molecular simulation study. Water Res 184, 116166.
- [62] Segad, M., Jönsson, B., Åkesson, T., Cabane, B., 2010. Ca/Na montmorillonite: structure, forces and swelling properties. Langmuir 26 (8), 5782–5790.
- [63] Hassan, M., Liu, Y., Naidu, R., Du, J., Qi, F., 2020. Adsorption of Perfluorooctane sulfonate (PFOS) onto metal oxides modified biochar. Environ Technol Innov 19, 100816.
- [64] Mehta, S., Kumar, S., Chaudhary, S., Bhasin, K., 2009. Effect of cationic surfactant head groups on synthesis, growth and agglomeration behavior of ZnS nanoparticles. Nanoscale Res Lett 4, 1197–1208.
- [65] de Carvalho Costa, T.C., Melo, J.D.D., Paskocimas, C.A., 2013. Thermal and chemical treatments of montmorillonite clay. Ceram Int 39 (5), 5063–5067.
- [66] Cottet, L., Almeida, C., Naidek, N., Viante, M., Lopes, M., Debacher, N., 2014. Adsorption characteristics of montmorillonite clay modified with iron oxide with respect to methylene blue in aqueous media. Appl Clay Sci 95, 25–31.
- [67] Zhao, F., Zhang, B., Feng, L., 2012. Preparation and magnetic properties of magnetite nanoparticles. Mater Lett 68, 112–114.
- [68] Zhang, K., Huang, J., Yu, G., Zhang, Q., Deng, S., Wang, B., 2013. Destruction of perfluorooctane sulfonate (PFOS) and perfluorooctanoic acid (PFOA) by ball milling. Environ Sci Technol 47 (12), 6471–6477.
- [69] Chotiradsirikun, S., Guo, R., Bhalla, A.S., Manuspiya, H., 2021. Novel synthesis route of porous clay heterostructures via mixed surfactant template and their dielectric behavior. J Porous Mater 28, 117–128.
- [70] Grieco, S.A., Chang, J., Maio, E.Y., Hwang, M., 2021. Comparing conventional and emerging adsorbents for per- and polyfluoroalkyl substances: kinetic, equilibrium, and column experiments. AWWA Water Sci 3 (6), e1256.
- [71] Huang, Y, Zhang, L, Ran, L, 2022. Total Organic Carbon Concentration and Export in a Human-Dominated Urban River: A Case Study in the Shenzhen River and Bay Basin. Water 14, 2102.
- [72] McCabe, K.M., Smith, E.M., Lang, S.Q., Osburn, C.L., Benitez-Nelson, C.R., 2021. Particulate and dissolved organic matter in stormwater runoff influences oxygen demand in urbanized headwater catchments. Environ Sci Technol 55 (2), 952–961.
- [73] Chen, M., Zeng, G., Zhang, J., Xu, P., Chen, A., Lu, L., 2015. Global landscape of total organic carbon, nitrogen and phosphorus in lake water. Sci Rep 5 (1), 15043.
- [74] Parker, B.A., Kanalos, C.A., Radniecki, T.S., Massey Simonich, S.L., Field, J.A., 2023. Evaluation of sorbents and matrix effects for treating heavy metals and perand polyfluoroalkyl substances as co-contaminants in stormwater. Environ Sci: Water Res Technol 9 (12), 3281–3289.
- [75] Pritchard, J.C., Cho, Y.M., Hawkins, K.M., Spahr, S., Higgins, C.P., Luthy, R.G., 2023. Predicting PFAS and hydrophilic trace organic contaminant transport in black carbon-amended engineered media filters for improved stormwater runoff treatment. Environ Sci Technol 57 (38), 14417–14428.
- [76] Ray, J.R., Shabtai, I.A., Teixidó, M., Mishael, Y.G., Sedlak, D.L., 2019. Polymer-clay composite geomedia for sorptive removal of trace organic compounds and metals in urban stormwater. Water Res 157, 454–462.
- [77] Borthakur, A., Das, T.K., Zhang, Y., Libbert, S., Prehn, S., Ramos, P., Dooley, G., Blotevogel, J., Mahendra, S., Mohanty, S.K., 2022. Rechargeable stormwater biofilters: in situ regeneration of PFAS removal capacity by using a cationic polymer, polydiallyldimethylammonium chloride. J Clean Prod 375, 134244.
- [78] Das, P., Árias, E. V.A., Kambala, V., Mallavarapu, M., Naidu, R., 2013. Remediation of perfluorooctane sulfonate in contaminated soils by modified clay adsorbent—a risk-based approach. Water, Air, Soil Pollut 224 (12), 1–14.